

Letter

A New Design of a Thin-Film Thermoelectric Device Based on Multilayer-Structure Module

Tianbao Chen, Zhuanghao Zheng, Guangxing Liang  and Ping Fan *

Shenzhen Key Laboratory of Advanced Thin Films and Applications, College of Physics and Optoelectronic Engineering, Shenzhen University, Shenzhen 518060, China; chentianbao@caihuang.com (T.C.); zhengzh@szu.edu.cn (Z.Z.); lgx@szu.edu.cn (G.L.)

* Correspondence: fanping@szu.edu.cn

Received: 21 April 2020; Accepted: 18 May 2020; Published: 21 May 2020



Abstract: In this work, a novel multilayer structure thin-film thermoelectric device is proposed for preparing a high performance generator. The result shows that the output voltage of the three-layer thin-film device has a linear increasing trend with the increasing temperature difference. Additionally, the device was also tested as a laser power measurement and displays that it has good sensitivity. Moreover, we also fabricated the multilayer device based on the present three-layer structure. It improves upon the similar output prosperities, confirming that the present multilayer structure thin-film thermoelectric device can be considered for preparing high performance micro-self-powered sources and sensors.

Keywords: thermoelectric; thin film; multilayer; device

1. Introduction

Thermoelectric (TE) technology can convert heat into electricity directly and it has many advantages, such as being environmental friendly, having low-cost operation and good reliability, and so on [1]. So, this technology has attracted much attention due to its many advantages and wide applications [2]. Recently, with the development of micro-electronics and an increasing demand for sustainable energy harvesting, high power density TE devices that are micro-sized and light-weight have become the subject of rapidly growing interest [3,4]. Compared with traditional brittle and rigid TE devices, a micro TE device is essential to obtain low temperatures such as that of the human body or flexible electronic devices, thus, minimizing heat loss and achieving highly efficient energy conversion [5]. Additionally, the integration of a TE device into the micro-system can act as the self-powered source, cooler, or sensor, and has significant potential for practical application. Thus, motivated by these intriguing prospects, considerable effort has been devoted to exploring micro-TE devices in the past decade [6–10]. Among many of the reports, micro-TE devices fabricated based on thin-film technology has been widely studied due to the free-standing thin-film thermoelectric materials which are always preferred to obtain optimum device configurations. It is because they can be easily transferred onto any substrate, enabling remarkable improvements in efficiency by reducing thermal energy losses [11]. Moreover, low-dimensional thin-film materials can achieve a very high Dimensionless thermoelectric figure of merit (ZT) value, leading to a high efficiency TE device [12]. For instance, Venkatasubramanian et al. [13] achieved a very high ZT value material of about 2.4 by using a superlattice structure. Then, Chowdhury et al. [14] made a thin-film TE device with the same concept, and fabricated it into state-of-the-art electronic packages with cooling to a high ($\sim 1300 \text{ Wcm}^{-2}$) heat flux. Tian et al. [15] prepared an organic superlattices generator with very high power density of 2.5 Wm^{-2} which is almost one hundred times higher than the others.

thickness of 2 mm and a surface roughness of <10 nm as the substrate. The Seebeck coefficient and electrical conductivity of the thin films were measured by the simultaneous determination of Seebeck coefficient and electrical conductivity system (SBA458). The detail preparing parameters and properties of the thin films are listed in Table 1. As shown in Table 1, the Seebeck coefficient is negative and the absolute value is $28 \mu\text{V K}^{-1}$ for the NiCu thin film, while a positive value of $15 \mu\text{V K}^{-1}$ is observed for NiCr thin film. Therefore, a prospective thermo-power with one pair of PN leg of the device is about $43 \mu\text{V K}^{-1}$. Both the NiCr and NiCu thin film have very high electrical conductivity, thus leading to low-contact resistance after connecting. The prepared SiO_2 layer has very low-electrical conductivity. Then, the double-layer films as “NiCr/ SiO_2 ” and “NiCu/ SiO_2 ” were prepared. The cross-sections of those thin films were examined and shown in Figure 2a by using a scanning electron microscopy (Zeiss supra 55). It can be found that the prepared double-layer thin films have good adhesion characteristics and few interface defects between the layers. Additionally, the cross-sections of these thin films after being heated to 400 K, in Figure 2b, display that all the thin films have few changes. It indicates the good thermal stability of the thin films we fabricated. At the same time, we also measure the resistance between the TE thin films and insulating layer shown in Figure 2c. The insert table in Figure 2c shows the influence of the SiO_2 thickness on the resistance. It displays that the resistance increases from about 100Ω to over $20 \text{M}\Omega$ when the thickness increases from ~ 200 nm to ~ 400 nm, which is sufficient for the blocked level to ensure the electrons and holes can only migrate according to the temperature gradient in the TE thin films.

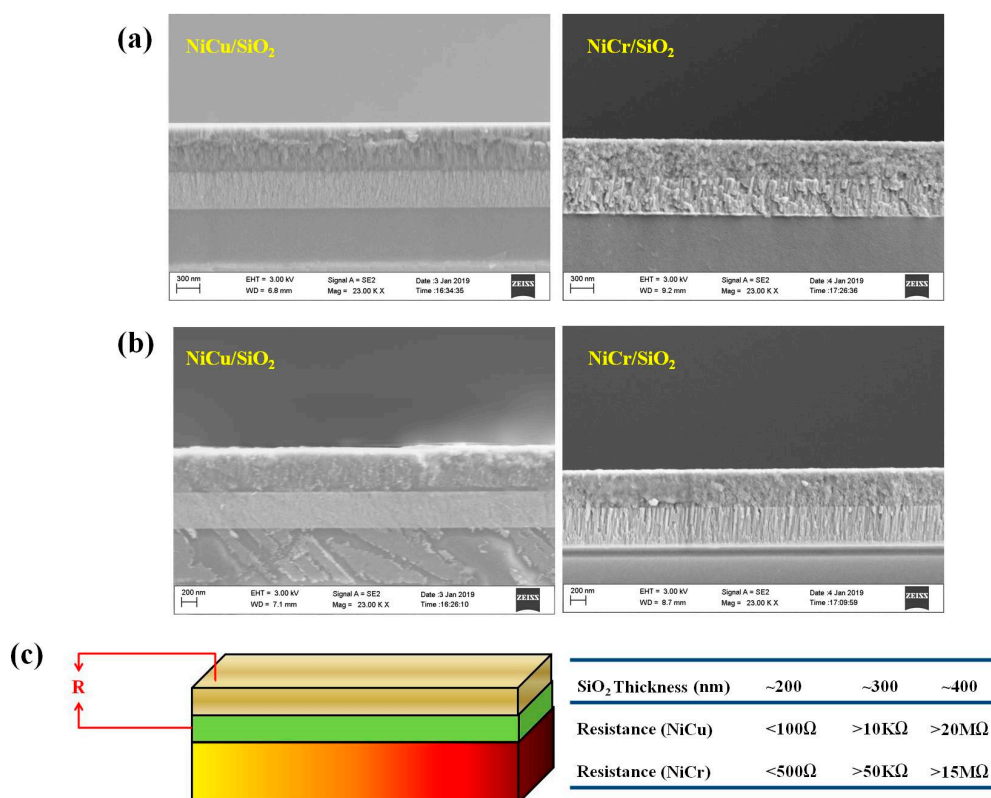


Figure 2. (a) The cross-section images of NiCu/ SiO_2 and NiCr/ SiO_2 thin films; (b) The cross-section images of NiCu/ SiO_2 and NiCr/ SiO_2 thin films after heating; and (c) The resistance between the TE thin films and SiO_2 .

Table 1. The detail preparing parameters and properties of the thin films.

	Sputtering Power	Ar Flow	O ₂ Flow	Thickness	Seebeck Coefficient	Electrical Conductivity
NiCu	100 W	40 sccm	—	370 nm	−28 μV K ^{−1}	15,300 Sm ^{−1}
NiCr	90 W	30 sccm	—	413 nm	15 μV K ^{−1}	14,000 Sm ^{−1}
SiO ₂	150 W	30 sccm	5 sccm	563 nm	—	<0.1 Sm ^{−1}

The TFTED with three-layer structure as “NiCr–SiO₂–NiCu” was fabricated and a schematic representation of the process is shown in Figure 3a. At first, the p-type thin film “leg” was deposited on the glass substrate and the thickness was around 400 nm. Then, the SiO₂ layer was deposited onto the P-type thin film with a mask which covered one side of the TE leg, leaving a connecting end. After that, the N-type thin film “leg” with the similar thickness as the P-type thin film was then deposited onto the SiO₂ layer, and the TE thin films were connected by the reserved side, thus forming the PN junction. The output voltages and short-circuit currents of the device were measured in normal atmosphere with a Keithley 2400 as a function of the temperature difference between hot and cold sides. Figure 3b shows the open output voltage (V_o) of the TFTED with a single PN junction as a function of temperature difference, ΔT . The imposed temperature gradient is parallel to the length of the TFTED leg. The result reveals that the V_o of the device increases linearly with the increasing temperature difference. The linear fit of the experimental data yields a Seebeck coefficient of about 45 $\mu\text{V K}^{-1}$, which agrees well with the prospective value of the PN junction of about 43 $\mu\text{V K}^{-1}$. The cross-sectional image measured by SEM was insert in Figure 3b, showing that all of the thin film layers has good adhesion characteristics and few interface defects between the layers. Besides, no obvious contact defect can be seen from the connecting side of the P-type and N-type layer. Furthermore, a TE device is favorable for highly sensitive detector applications. Therefore, a laser power measurement application using this multilayer device was also tested as shown in Figure 3c. The Kethley 2400 and a laser which used the continuous monitoring mode with an interval time of 0.05 s were employed. The continuous response of the TFTED was measured by the laser beam with respective 50 s interval irradiating the connecting region of the device as “on” and “off”, and the irradiation time was 25 s. The output signal as the function of the testing time is also shown in Figure 3c. It can be seen that the voltage increases rapidly in response to the “on” state and has the maximum output voltage about 0.4 mV, suggesting that the thermal gradient is about 10 K ($0.4 \text{ mv}/0.45 \text{ uvK} - 1 = 8.89 \text{ K}$). Especially, the rise time of reaching the maximum voltage for each laser beam is about 2–3 s and this TFTED had stable output voltage when the laser beam continued irradiating. This response time is shorter than the commercial laser power detector which needs over 5 s to achieve a stable value. Additionally, we also measured the response time of traditional bulk thermocouples, fabricated with NiCu and NiCr by using the same method. It displays that the response time is about 50% higher than that of our prepared thin film device, indicating the TFTED can be considered for using as a fast response sensor.

In order to further investigate the reliability of the multilayer structure, the TFTED was fabricated by using different TE materials. The N-type Bi and P-type Sb, which have higher TE properties and very weak temperature dependence compared to the traditional Ni-based materials, were used for fabricating the TFTED. In addition, the N-type Bi₂Te₃ and P-type Sb₂Te₃ were also employed due to their good thermoelectric performance at room temperature. The room-temperature TE properties of Bi, Sb, Bi₂Te₃, and Sb₂Te₃ prepared by magnetron sputtering disposition are shown in Table 2. Besides one PN junction, the Ni-based and Bi₂Te₃/Sb₂Te₃ based TFTEDs with seven layers, which owned two thermocouples, were also fabricated to contrast with the signal PN junction. Figure 4 shows the open output voltage (V_o) of the devices as a function of ΔT for the devices. It can be seen from Figure 4 that the output voltage of the seven-layer Ni-based device exhibits a linear increasing trend with the increasing ΔT and the value is about two times that of the device with a single thermocouple as shown in Figure 3, indicating that the multilayer structure devices have good stability. Similarly, the device with a single Bi/Sb PN junction also shows the linear increasing trend with the increasing

ΔT . It has a higher output voltage than that of the device fabricated with Ni-based device due to their higher Seebeck coefficient. Assuredly, the $\text{Bi}_2\text{Te}_3/\text{Sb}_2\text{Te}_3$ based device has the maximum output voltage among the devices. The maximum output voltage increases with the increasing of ΔT and doubles after adding a pair of thermocouples. All of these results suggest that the multilayer structure is promising for preparing high integration devices and applications to exploit various practically available heat sources.

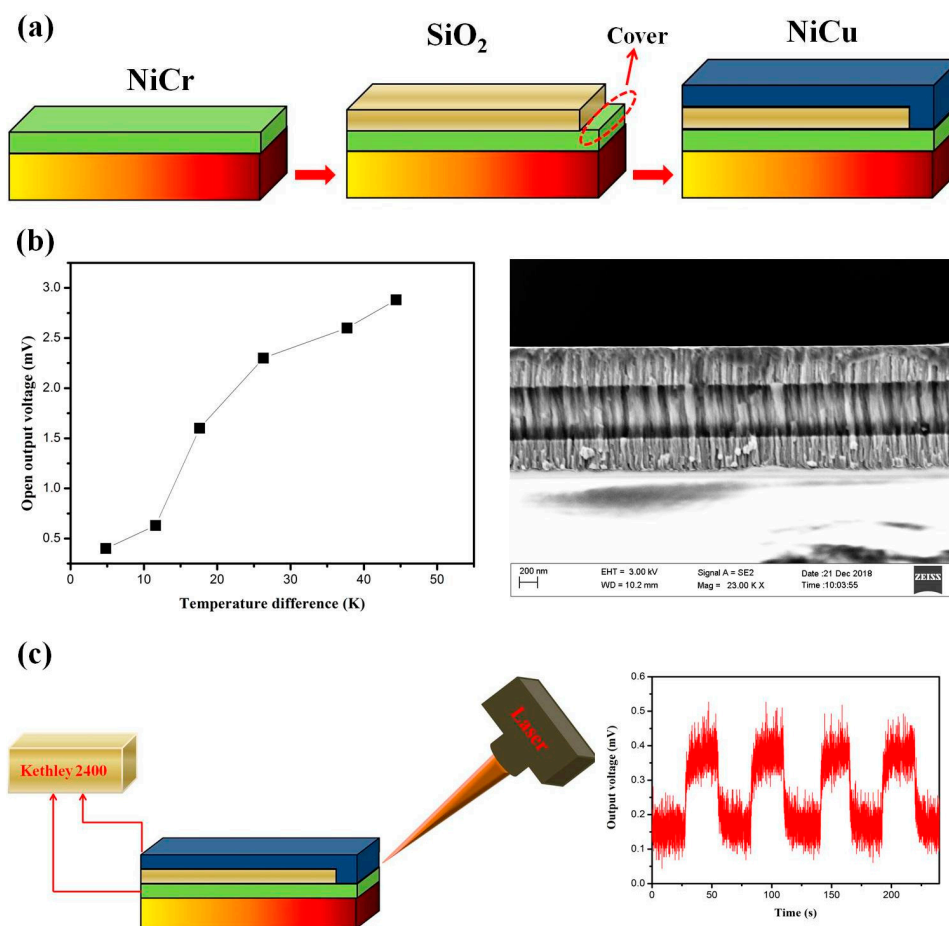


Figure 3. (a) The preparing process of the three-layer TFTED; (b) The open output voltage of the TFTED as function of temperature difference and the cross-section image; and (c) An illustration of the laser power measurement application by using TFTED and the continuous response testing.

Table 2. The room-temperature thermoelectric properties of the thin films.

	Seebeck Coefficient	Electrical Conductivity
Sb	47 $\mu\text{V K}^{-1}$	7700 Sm^{-1}
Bi	-33 $\mu\text{V K}^{-1}$	6500 Sm^{-1}
Sb_2Te_3	125 $\mu\text{V K}^{-1}$	4700 Sm^{-1}
Bi_2Te_3	-97 $\mu\text{V K}^{-1}$	4300 Sm^{-1}

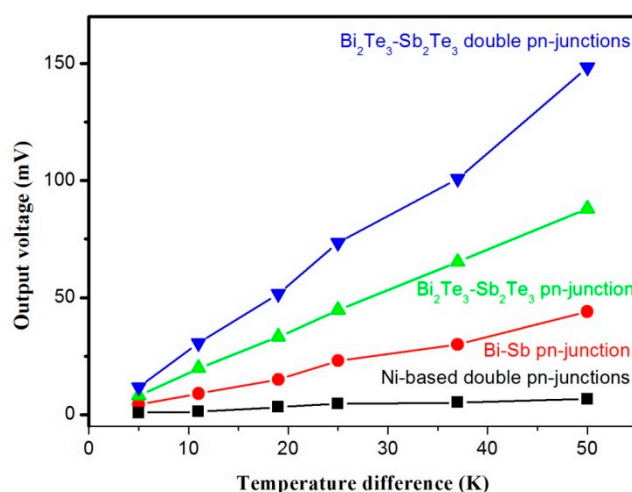


Figure 4. The open output voltage of the TFTED with various materials as function of temperature difference.

3. Conclusions

A novel multilayer structure design is used for preparing a thin-film thermoelectric device. It is shown that the output voltage of all of the prepared thin-film devices have a linear increasing trend with the increasing temperature difference, indicating the reliability of the multilayer structure. The laser sensor test results show that the prepared thin-film device has high sensitivity and a lower response time than that of the commercial laser power detector. Thus, our multilayer structure is a promising new structure that can be used for fabricating high integration and high-performance thin-film devices.

Author Contributions: T.C.; methodology, Z.Z. and G.L.; formal analysis, T.C. and P.F.; P.F. supervision. All authors have read and agreed to the published version of the manuscript.

Funding: This research was funded by National Natural Science Foundation of China (No. 11604212) and Shenzhen Key Lab Fund (ZDSYS 20170228105421966).

Conflicts of Interest: The authors declare no conflict of interest.

References

- Dresselhaus, M.S.; Thomas, I.L. Alternative energy technologies. *Nature* **2001**, *414*, 332. [[CrossRef](#)] [[PubMed](#)]
- Chu, S.; Majumdar, A. Opportunities and challenges for a sustainable energy future. *Nature* **2012**, *488*, 294. [[CrossRef](#)] [[PubMed](#)]
- Bahk, J.H.; Fang, H.; Yazawa Shakouri, A. Flexible thermoelectric materials and device optimization for wearable energy harvesting. *J. Mater. Chem. C* **2015**, *3*, 10362. [[CrossRef](#)]
- Kim, S.K.; We, J.H.; Cho, B.J. A wearable thermoelectric generator fabricated on a glass fabric. *Energy Environ. Sci.* **2014**, *7*, 1959. [[CrossRef](#)]
- Culebras, M.; Cho, C.; Kreckler, M.; Smith, R.; Song, Y.; Goómez, C.M.; Cantarero, A.; Grunlan, J.C. High thermoelectric power factor organic thin films through combination of nanotube multilayer assembly and electrochemical polymerization. *ACS Appl. Mater. Interfaces* **2017**, *9*, 6306. [[CrossRef](#)] [[PubMed](#)]
- Fan, P.; Zheng, Z.H.; Li, Y.Z.; Lin, Q.Y.; Luo, J.T.; Liang, G.X.; Cai, X.M.; Zhang, D.P.; Ye, F. Low-cost flexible thin film thermoelectric generator on zinc based thermoelectric materials. *Appl. Phys. Lett.* **2015**, *106*, 073901. [[CrossRef](#)]
- Lu, Z.; Layani, M.; Zhao, X.; Tan, L.P.; Sun, T.; Fan, S.; Yan, Q.; Magdassi, S.; Hng, H.H. Fabrication of flexible thermoelectric thin film devices by inkjet printing. *Small* **2014**, *17*, 3551. [[CrossRef](#)] [[PubMed](#)]
- Chen, Y.; Zhao, Y.; Liang, Z. Solution processed organic thermoelectrics: Towards flexible thermoelectric modules. *Energy Environ. Sci.* **2015**, *8*, 401. [[CrossRef](#)]
- Zhu, W.; Deng, Y.; Cao, L.L. Light-concentrated solar generator and sensor based on flexible thin-film thermoelectric device. *Nano Energy* **2017**, *34*, 463. [[CrossRef](#)]

10. Pan, Y.; Tagliabue, G.; Eghlidi, H.; Höller, C.; Dröscher, S.; Hong, G.; Poulidakos, D. A rapid response thin-film plasmonic-thermoelectric light detector. *Sci. Rep.* **2016**, *6*, 37564. [[CrossRef](#)] [[PubMed](#)]
11. Savage, N. Thermoelectric coolers. *Nature Pho.* **2009**, *3*, 541. [[CrossRef](#)]
12. Chen, G.; Dresselhaus, M.S.; Dresselhaus, G.; Fleurial, J.P.; Caillat, T. Recent developments in thermoelectric materials. *Inter. Mater. Rev.* **2003**, *48*, 4513. [[CrossRef](#)]
13. Venkatasubramanian, R.; Siivola, E.; Colpitts, T.; O'Quinn, B. Thin-film thermoelectric devices with high room-temperature figures of merit. *Nature* **2001**, *413*, 597. [[CrossRef](#)] [[PubMed](#)]
14. Chowdhury, I.; Prasher, R.; Lofgreen, K.; Chrysler, G.; Narasimhan, S.; Mahajan, R.; Koester, D.; Alley, R.; Venkatasubramanian, R. On-chip cooling by superlattice-based thin-film thermoelectrics. *Nat. Nanotechnol.* **2009**, *4*, 235. [[CrossRef](#)]
15. Tian, R.; Wan, C.; Wang, Y.; Wei, Q.; Ishida, T.; Yamamoto, A.; Tsuruta, A.; Shin, W.; Li, S.; Koumoto, K. A solution-processed TiS₂/organic hybrid superlattice film towards flexible thermoelectric devices. *J. Mater. Chem.* **2017**, *A5*, 564. [[CrossRef](#)]



© 2020 by the authors. Licensee MDPI, Basel, Switzerland. This article is an open access article distributed under the terms and conditions of the Creative Commons Attribution (CC BY) license (<http://creativecommons.org/licenses/by/4.0/>).